STUDY OF RESISTIVE-WALL EFFECTS ON SOLEIL

R. Nagaoka, Synchrotron SOLEIL, Gif-sur-Yvette, France

Abstract

The paper describes the way the machine data on the resistive-wall is organised and the impact of the resistive-wall evaluated for the SOLEIL storage ring. The instability is expected to appear from low beam currents in both transverse planes. The degree of incoherent tune shift arising from the chamber cross section asymmetry is estimated in multibunch as well as in single bunch. It is found that the NEG coating adopted to enhance the vacuum pumping performance nearly doubles the reactive part of the impedance.

INTRODUCTION

The presence of low-gap chambers for insertion devices, along with a relatively small vertical gap of 25 mm chosen for the standard vacuum chambers, implies a significant influence of the resistive-wall (RW) on the beam in the future SOLEIL storage ring. Unlike previous machines in which the RW predominantly caused transverse instability in multibunch, it is expected to affect the coherent single bunch motion as much as the broadband impedance. Furthermore, its impact on the incoherent motion is likely to be non-negligible, due to the ring being composed mostly of low gap non-circular chambers, which in turn may interfere with the coherent instability in a non-trivial manner. With enhanced sensitivity to RW, the impact of metallic coating on the chamber surface, either to improve the wall conductivity or the vacuum pumping capacity, needs also be studied.

MACHINE DATA ORGANISATION

Although the RW impedance is generally known analytically, an accurate evaluation of its magnitude, as well as its product with the beta function over the entire machine, may not be simple when both the vacuum chamber and the optics vary rapidly around the ring.

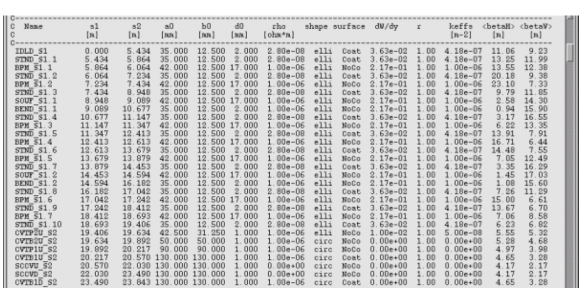

Name	s1 [m]	s2 [m]	a0 [mm]	b0 [mm]	d0 [mm]	rho [ohm*m]	shape	surface	dW/dy	r	keffs [m-2]	<betaH> [m]	<betaV> [m]
IDLD_S1	0.000	5.434	35.000	12.500	2.000	2.80e-08	elli	Coat	3.63e-02	1.00	4.18e-07	11.06	9.23
STND_S1.1	5.434	5.864	35.000	12.500	2.000	2.80e-08	elli	Coat	3.63e-02	1.00	4.18e-07	13.25	11.99
BPM_S1.1	5.864	6.064	42.000	12.500	17.000	1.00e-06	elli	NoCo	2.17e-01	1.00	1.00e-06	13.55	12.38
STND_S1.2	6.064	7.234	35.000	12.500	2.000	2.80e-08	elli	Coat	3.63e-02	1.00	4.18e-07	20.18	9.38
BPM_S1.2	7.234	7.434	42.000	12.500	17.000	1.00e-06	elli	NoCo	2.17e-01	1.00	1.00e-06	23.10	7.33
STND_S1.3	7.434	8.948	35.000	12.500	2.000	2.80e-08	elli	Coat	3.63e-02	1.00	4.18e-07	9.79	11.85
SOUF_S1.1	8.948	9.089	42.000	12.500	17.000	1.00e-06	elli	NoCo	2.17e-01	1.00	1.00e-06	2.58	14.30
BEND_S1.1	9.089	10.677	35.000	12.500	2.000	1.00e-06	elli	NoCo	2.17e-01	1.00	1.00e-06	0.94	15.90
STND_S1.4	10.677	11.147	35.000	12.500	2.000	2.80e-08	elli	Coat	3.63e-02	1.00	4.18e-07	3.17	16.55
BPM_S1.3	11.147	11.347	42.000	12.500	17.000	1.00e-06	elli	NoCo	2.17e-01	1.00	1.00e-06	6.22	13.35
STND_S1.5	11.347	12.413	35.000	12.500	2.000	2.80e-08	elli	Coat	3.63e-02	1.00	4.18e-07	13.91	7.91
BPM_S1.4	12.413	12.613	42.000	12.500	17.000	1.00e-06	elli	NoCo	2.17e-01	1.00	1.00e-06	16.71	6.44
STND_S1.6	12.613	13.679	35.000	12.500	2.000	2.80e-08	elli	Coat	3.63e-02	1.00	4.18e-07	14.48	7.55
BPM_S1.5	13.679	13.879	42.000	12.500	17.000	1.00e-06	elli	NoCo	2.17e-01	1.00	1.00e-06	7.05	12.49
STND_S1.7	13.879	14.453	35.000	12.500	2.000	2.80e-08	elli	Coat	3.63e-02	1.00	4.18e-07	3.35	16.29
SOUF_S1.2	14.453	14.594	42.000	12.500	17.000	1.00e-06	elli	NoCo	2.17e-01	1.00	1.00e-06	1.45	17.03
BEND_S1.2	14.594	16.182	35.000	12.500	2.000	1.00e-06	elli	NoCo	2.17e-01	1.00	1.00e-06	1.08	15.60
STND_S1.8	16.182	17.042	35.000	12.500	2.000	2.80e-08	elli	Coat	3.63e-02	1.00	4.18e-07	7.26	11.29
BPM_S1.6	17.042	17.242	42.000	12.500	17.000	1.00e-06	elli	NoCo	2.17e-01	1.00	1.00e-06	15.00	6.61
STND_S1.9	17.242	18.412	35.000	12.500	2.000	2.80e-08	elli	Coat	3.63e-02	1.00	4.18e-07	13.67	6.70
BPM_S1.7	18.412	18.693	42.000	12.500	17.000	1.00e-06	elli	NoCo	2.17e-01	1.00	1.00e-06	7.06	8.58
STND_S1.10	18.693	19.406	35.000	12.500	2.000	2.80e-08	elli	Coat	3.63e-02	1.00	4.18e-07	6.23	6.82
CVTP2U_S2	19.406	19.634	42.500	31.250	1.000	1.00e-06	elli	NoCo	1.00e-02	1.00	5.00e-08	5.55	5.32
CVTB2U_S2	19.634	19.892	50.000	50.000	1.000	1.00e-06	circ	NoCo	0.00e+00	1.00	0.00e+00	5.28	4.68
CVTP1U_S2	19.892	20.217	90.000	90.000	1.000	1.00e-06	circ	NoCo	0.00e+00	1.00	0.00e+00	4.97	3.98
CVTB1U_S2	20.217	20.570	130.000	130.000	1.000	1.00e-06	circ	Coat	0.00e+00	1.00	0.00e+00	4.65	3.28
SCCVU_S2	20.570	22.030	130.000	130.000	1.000	0.00e+00	circ	NoCo	0.00e+00	1.00	0.00e+00	4.17	2.17
SCCVD_S2	22.030	23.490	130.000	130.000	1.000	0.00e+00	circ	NoCo	0.00e+00	1.00	0.00e+00	4.17	2.17
CVTB1D_S2	23.490	23.843	130.000	130.000	1.000	1.00e-06	circ	Coat	0.00e+00	1.00	0.00e+00	4.65	3.28

Figure 1: File containing the machine data.

To be able to trace, as well, evolution of the machine impedance associated with chamber replacements, a systematic approach was adopted to evaluate RW effects in a consistent manner. A large machine file was prepared containing all the basic information related to the RW, piecewise for each chamber component around the ring. Data include cross section form, length, wall thickness, electric resistivity and average beta values over the component length. In addition, coating information as well as parameters specific to the incoherent tune shift, such as form factor and effective focusing strength, are entered (Fig. 1). These machine files are commonly used by codes developed to study different RW effects.

IMPACT OF COATING

The standard RW impedance formula assumes a circular beam pipe with infinite wall thickness. To take into account the metallic coating on the wall surface, we have employed A. Chao's formalism [1] to derive extended formulae longitudinally and transversely. They were found to agree numerically with those obtained by Burov and Lebedev in a different approach. They also derived expressions for flat chambers [2], which differ from the former by form factors of $\pi^2/12$ vertical and $\pi^2/24$ horizontal. Elliptical and rectangular chambers lie between the two extremities.

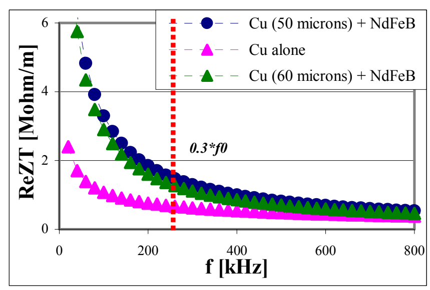

Figure 2: Transverse RW impedance for an in-vacuum undulator with Cu coating. The true case with Ni is expected to lie between the blue and green curves.

The formula was applied to in-vacuum undulators that have 50 µm thick Cu coating on the surface with 10 µm Ni in between Cu and NdFeB magnet blocks. While the Cu coating is found to well suppress the energy loss, its thickness is insufficient at the lowest betatron frequency that most strongly induces the RW instability (Fig. 2).

Triggered by the observation of an anomalous increase of the single bunch dipole mode detuning associated with installation of NEG coated aluminium chambers at Elettra [3], its impact was studied with the above two metallic layer model. The use of NEG coated Al chambers is envisaged for SOLEIL in all straight sections. Assuming the thickness of 1 µm and the resistivity of 25×10^{-8} Ωm, which is of Vanadium, the constituent material with the lowest resistivity, we find that the reactive part is nearly doubled, while the resistive part is roughly unchanged, in the frequency range up to ~10 GHz (Fig. 3). This feature is common transversely and longitudinally. The increase of the reactive part is in qualitative agreement with the observation.

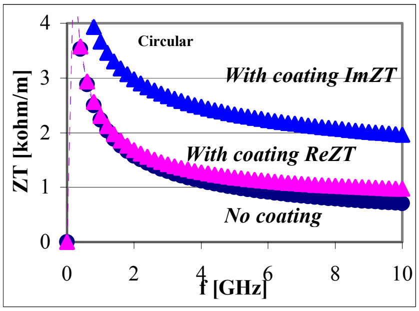

Figure 3: Transverse impedance with and without NEG coating.

Though the effective resistivity of NEG is not known, the impedance is found to saturate fast with increasing resistivity (Figs. 4a). This, along with the measurement of E. Plouviez finding ~ 1600×10^{-8} Ωm for NEG [4], would indicate that the result in Fig. 3 represents the plausible cases. The impedance also saturates fast with increasing thickness, correctly to the value determined by the coating material (Figs. 4b).

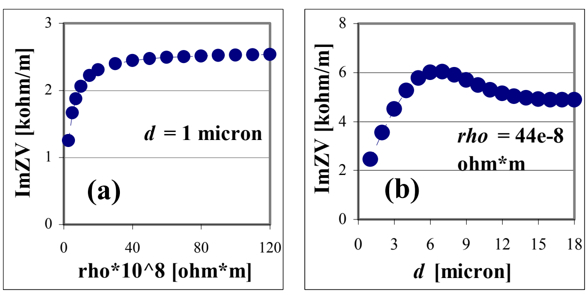

Figures 4: Dependence of the vertical impedance (calculated at 2 GHz) on the resistivity ρ (left) and the coating thickness d (right).

With all straight section coated with NEG, it follows that for SOLEIL, the NEG nearly doubles the total imaginary impedance as well, though the increased value is still roughly half of what it would have been had all the chambers been made in stainless steel. As long as the increase occurs only on the imaginary part, the resistive-wall instability is supposed to be unaffected. On the other hand, the threshold of the transverse mode coupling instability (TMCI) in single bunch may be seriously reduced. The latter is quantified in a later section.

Despite the qualitative agreement, the present model fails to reproduce the Elettra observation quantitatively by as much as an order of magnitude. Staying within the model, one is obliged to assume unreasonably large values for both the thickness and the resistivity. This discrepancy, along with an additional observation at ELETTRA suggesting a simultaneous increase of the real part of the impedance, may indicate that the origin may well be other than the model considered here. One good candidate would be the surface roughness, which is already known for NEG coated aluminium chambers. Collaboration is made with ELETTRA and the ESRF to analyse the ELETTRA observations.

RESISTIVE-WALL INSTABILITY

Instability thresholds were calculated in the frequency domain, by solving the Sacherer equation and equating the growth rate with that of the radiation damping. Only the uniform filling was considered. At zero chromaticity, the preferred value for the operation, unstable modes appear at around 30 mA vertically and 80 mA horizontally, whose number grow up to around 90 and 30, respectively (Fig. 5). The computation assumed no broadband (BB) impedance, which anyway has little effect at zero chromaticity.

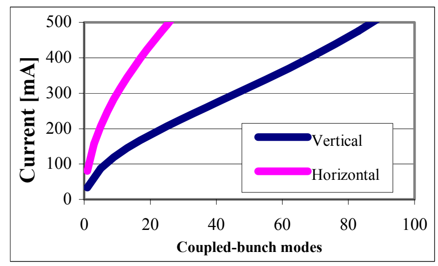

Figure 5: Number of unstable modes versus current at zero chromaticity.

To follow the dependence of the instability on the chromaticity ξ, the knowledge of BB impedance is important. Here, a set of broadband resonator (BBR) impedance, deduced from the ESRF case [5], was employed to investigate the more stringent vertical stability: $R_V\cdot\beta = 1.43$ MΩ, $f_{res} = 22$ GHz, Q=1. We note that the value of $R_V\cdot\beta$ is close to the estimated budget [6].

It turns out that the current does not rise favourably by increasing ξ (Fig. 6a). Namely, where the higher-order head-tails (m>0) are involved, the threshold current remains low. Interestingly, the number of unstable modes shows a minimum around ξ =0.1, where m=0 gets stabilised while m=1 is not yet unstable (Fig. 6b). Above this point, all coupled-bunch modes become unstable once m > 0 modes are excited by the BB impedance. Clearly there is an advantage to work at this minimum for the transverse feedback. The behaviour of m > 0 modes at ξ > 0, as well as the minimum described here were also observed in a study made earlier [7].

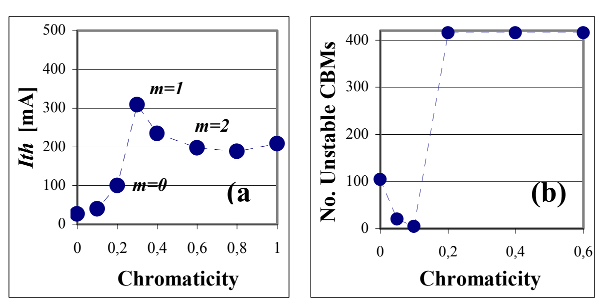

Figures 6: Dependence on the chromaticity (normalised). (Left) Vertical current threshold. (Right) Number of unstable modes. The computation includes the BBR described in the main text.

INCOHERENT TUNE SHIFT

Non-circular chambers with finite resistivity create current-dependent quadrupole fields [8], which generate incoherent betatron tune shifts. The scheme developed earlier by the author to quantify the effect [9] was improved as follows: On top of evaluating the chambers piecewise around the machine as already described, the focusing strength derived via the formulation of K. Yokoya [8] has now the time dependence according to A. Chao et al. [10]. Namely, the field diffusion is computed as an explicit function of the aperture, wall thickness, resistivity and time, thus eliminating the artificial parameter used earlier. Other details are found in Ref. 9.

Applying it to SOLEIL, tune shifts of as large as ~0.025 are found at 500 mA in uniform filling, horizontally and vertically (Fig. 8a). While the NEG coating is not expected to have any effect in multibunch as the zero frequency field dominates, for single bunch its contribution is taken into account, thanks to the relation in the horizontal impedance $(Z_H)_{incoherent} = -(Z_H)_{coherent}$ for flat chambers. The effective focusing strength felt by a particle in single bunch is then given by

$$< k_{effs} > = \frac{4\pi}{Q} \cdot \frac{1}{E/e} \int_0^{\infty} \tilde{\rho}(\omega)^2 \cdot \mathrm{Im}\, Z_H(\omega)\, d\omega, \qquad (1)$$

where Q denotes the total bunch charge, E, the beam energy, $\tilde{\rho}(\omega)$, the Fourier transform of the bunch density, and $Z_H(\omega)$ is the coherent horizontal impedance. The two-metallic layer impedance formula of Ref. 2 is used when considering the NEG coating. Tune shifts in single bunch are again found to be comparable in the two transverse planes. With NEG, they reach nearly 0.0035 at the nominal current of 10 mA (Fig. 8b).

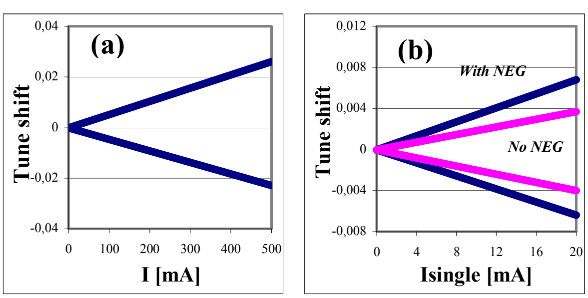

Figures 8: Calculated incoherent tune shift in multibunch (left) and single bunch (right). Negative shifts are vertical and vice versa for the horizontal.

The impact of resistive-wall on the coherent dipolar tune shift in single bunch is finally estimated. Tune shifts are computed as the sum of coherent and incoherent parts, both taking account the NEG effect. The results show that the NEG increases the dipolar detuning in both transverse planes (Figs. 9). With the synchrotron frequency being close to 6 kHz, a naïve estimate of the vertical TMCI threshold gives 14 mA without NEG, which is reduced to 8 mA with NEG. Clearly, the important contribution of numerical calculated BB impedance [6], must be added to make a more realistic estimate.

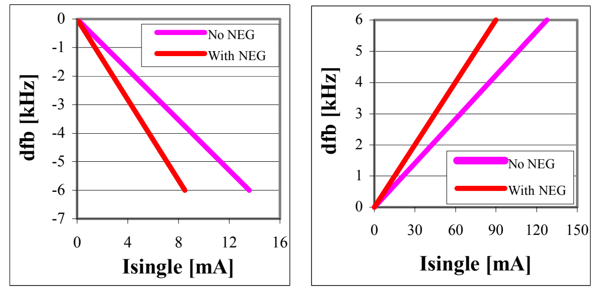

Figures 9: Calculated dipole mode detuning due to resistive-wall, vertical (left) and horizontal (right).

CONCLUSION

The detailed piecewise data on the RW and the optics around the ring constitutes the basis for a precise and systematic evaluation of the beam dynamics due to the RW. As its dominant contribution was confirmed in the impedance budget [6], the RW was shown to give by itself a significant effect for SOLEIL on the collective stability of multibunch and single bunch, both vertically and horizontally. Not only, but its impact on the incoherent tune shift was found to be non-negligible.

The study is to be extended to include the BB impedance numerically calculated. The beam filling dependence of the RW instability shall be explored in particular, as gaps in the filling have been found to give significant stabilisation in some machines. A multibunch tracking is to be performed for this purpose [5].

ACKNOWLEDGEMENT

R.N. wishes to thank M.P. Level and J.M. Filhol for helpful discussions on this work.

REFERENCES

[1] A. Chao, "Physics of Collective Beam Instabilities in High Energy Accelerators", Wiley & Sons, 1993.
[2] A. Burov and V. Lebedev "Transverse Resistive Wall Impedance for Multi-Layer Flat Chambers", EPAC 2002, Paris.
[3] E. Karantzoulis et al., Phys. Rev. ST-AB **6**, 030703 (2003).
[4] E. Pouviez, ESRF note, Diagnostics 02-03, 2002.
[5] R. Nagaoka, "Study of Resistive-Wall Instabilities with a Multi-bunch Tracking", EPAC 2002, Paris.
[6] R. Nagaoka, "Numerical Evaluation of Geometric Impedance for SOLEIL", this conference.
[7] A. Mosnier, SOLEIL conceptual design report (APD).
[8] K. Yokoya, Part. Acc., **41** (1993) 221.
[9] R. Nagaoka et al., "Incoherent Transverse Tune Shifts due to Resistive Low-Gap Chambers", EPAC 2002, Paris.
[10] A. Chao et al., Phys. Rev. ST-AB **5**, 111001 (2002).